Contrib. Mineral. Petrol. 70, 407–419 (1979)

Contributions to Mineralogy and Petrology

Zircon Saturation in Felsic Liquids: Experimental Results and Applications to Trace Element Geochemistry

E. Bruce Watson

Department of Geology, Rensselaer Polytechnic Institute, Troy, New York 12181, USA

Abstract. Hydrothermal experiments were carried out at 2 kbar water pressure, 700°–800° C, with the objective of determining the level of dissolved Zr required for precipitation of zircon from melts in the system SiO_2–Al_2O_3–Na_2O–K_2O. The saturation level depends strongly upon molar $(Na_2O+K_2O)/Al_2O_3$ of the melts, with remarkably little sensitivity to temperature, SiO_2 concentration, or melt Na_2O/K_2O. For peraluminous melts and melts lying in the quartz-orthoclase-albite composition plane, less than 100 ppm Zr is required for zircon saturation. In peralkaline melts, however, zircon solubility shows pronounced, apparently linear, dependence upon $(Na_2O+K_2O)/Al_2O_3$, with the amount of dissolvable Zr ranging up to 3.9 wt.% at $(Na_2O+K_2O)/Al_2O_3=2.0$. Small amounts (1 wt.% each) of dissolved CaO and Fe_2O_3 cause a 25% relative reduction of zircon solubility in peralkaline melts.

The main conclusion regarding zirconium/zircon behavior in nature is that any felsic, non-peralkaline magma is likely to contain zircon crystals, because the saturation level is so low for these compositions. Zircon fractionation, and its consequences to REE, Th, and Ta abundances must, therefore, be considered in modelling the evolution of these magmas. Partial melting in any region of the Earth's crust that contains more than ~100 ppm Zr will produce granitic magmas whose Zr contents are buffered at constant low (< 100 ppm) values; unmelted zircon in the residual rock of such a melting event will impart to the residue a characteristic U- or V-shaped REE abundance pattern. In peralkaline, felsic magmas such as those that form pantellerites and comendites, extreme Zr (and REE, Ta) enrichment is possible because the feldspar fractionation that produces these magmas from non-peralkaline predecessors does not drive the melt toward saturation in zircon.

Zircon solubility in felsic melts appears to be controlled by the formation of alkali-zirconosilicate complexes of simple (2:1) alkali oxide: ZrO_2 stoichiometry.

Introduction

Zircon is an ubiquitous minor mineral whose presence in magmas or in regions of magma production may have profound effects upon the distribution of several important trace elements in igneous rock series. In addition to its dominant role in zirconium and hafnium geochemistry, for example, zircon may have a significant influence on the behavior of rare earth elements (Nagasawa, 1970). At the present time, our understanding of the factors that control zircon crystallization is not sufficient to allow quantitative consideration of its effects on these trace elements. We have, in particular, only vagure knowledge of the temperatures and Zr concentrations required for zircon to crystallize from magmas, and any dependence upon magma composition variables is poorly understood. Detailed studies of rocks have provided some insight into these problems. Poldervaart (1956), for example, summarized petrographic arguments for the generally early crystallization of zircon from magmas ranging in composition from basaltic to granitic. A probable exception to this pattern of early zircon appearance was emphasized by Siedner (1965), who suggested that high zircon solubility in strongly alkaline magmas may result in late and only minor zircon crystallization (see also Wager and Mithchell, 1951; Goldschmidt, 1954; Chao and Fleischer, 1960). From his observations of zircon abundances and zirconium concentrations in granites of widely ranging alkalinity, Bowden (1966) concluded that zircon solubility does in fact increase with increasing magma alkalinity as gauged by the alkali/aluminium ratio.

Existing experimental data on zircon crystallization include those of Larsen (1973) for a water-satu-

0010-7999/79/0070/0407/$02.60

Table 1. Bulk compositions of starting materials (excluding ZrO_2)

	Series with variable $(Na_2O+K_2O)/Al_2O_3$													
	M		PM		P		PPK		PK		KPK		K	
	mol%	wt.%	mol%	wt.%	mol%	wt.%	mol%	wt.%	mol%	wt.%	mol%	wt.%	mol%	wt.%
SiO_2	84.13	77.80	84.13	78.07	84.13	78.33	84.13	78.55	84.13	78.77	84.13	79.00	84.13	79.23
Al_2O_3	9.52	14.94	8.73	13.75	7.94	12.55	7.28	11.53	6.62	10.52	5.96	9.50	5.29	8.46
Na_2O	3.94	3.76	4.43	4.24	4.92	4.73	5.33	5.13	5.74	5.54	6.15	5.96	6.56	6.37
K_2O	2.41	3.49	2.71	3.94	3.01	4.39	3.27	4.79	3.52	5.17	3.77	5.55	4.02	5.94
Alk/Al	0.67		0.82		1.00		1.18		1.40		1.66		2.00	
Na/K	1.63		1.63		1.63		1.63		1.63		1.63		1.63	

	Series with variable SiO_2									
	LS		LS1		LS2		LS3		LS4	
	mol%	wt.%	mol%	wt.%	mol%	wt.%	mol%	wt.%	mol%	wt.%
SiO_2	75.46	67.99	77.15	69.99	78.82	72.00	80.46	73.99	82.08	75.99
Al_2O_3	11.25	17.20	10.48	16.13	9.71	15.05	8.96	13.98	8.21	12.90
Na_2O	8.25	7.67	7.68	7.19	7.12	6.71	6.57	6.23	6.02	5.75
K_2O	5.05	7.13	4.70	6.69	4.36	6.24	4.02	5.80	3.69	5.36
Alk/Al	1.18		1.18		1.18		1.18		1.18	
Na/K	1.63		1.63		1.63		1.63		1.63	

rated, haplogranitic composition ($Q_{45}Ab_{15}Or_{40}$) at 830° C and 2 kbar, and those of Dietrich (1968) for Q–Or–Ab and Q–Or–Ab+$Na_2Si_2O_5$ or NaF compositions at 650°–900° C and 1 kbar water pressure. For the particular composition and experimental conditions that he used, Larsen found that only 57 ppm Zr is required to saturate the melt in zircon. Dietrich obtained qualitatively similar values for zircon saturation in Q–Or–Ab sompositions, but, in accord with petrographic observations, concluded that peralkaline liquids (containing $Na_2Si_2O_5$ or NaF) could dissolve considerably more zirconium. The author emphasized, however, that equilibrium may not have been attained in many of his runs.

This paper describes an experimental study designed to measure quantitatively and systematically the effects of temperature and composition variables upon the solubility of zircon in simple but geologically meaningful silicate melts. Because it is generally the late differentiates of most rock series that show evidence of zircon fractionation (Nockolds and Allen, 1953, p. 138), the study was confined to felsic compositions. In view of the consensus that magma alkalinity affects zircon solubility (see references noted above), the ratio $(Na_2O+K_2O)/Al_2O_3$ was the composition variable of primary interest. The significance of the experimental results to trace element models of the generation and evolution of felsic magmas is discussed, and the dependence of zircon solubility on liquid composition is explained in terms of silicate melt structure.

Experimental System and Methods

Bulk Compositions

The minimum melting composition in the 'granite' system $KAlSi_3O_8$(Or)–$NaAlSi_3O_8$(Ab)–SiO_2(Q) at 2 kbar water pressure was chosen as a starting point for the zircon saturation experiments. This minimum lies at $Or_{26}Ab_{40}Q_{34}$, for which composition the liquidus is 690° C and the melt contains about 6 wt.% dissolved H_2O at the run temperatures used (Tuttle and Bowen, 1958). In order to examine the effect of variations in $(Na_2O+K_2O)/Al_2O_3$ on zircon solubility, excursions from the Or–Ab–Q minimum toward both peralkaline and peraluminous compositions were made. To this end, a series of bulk compositions was prepared in which each mixture had the same molar SiO_2 and Na_2O/K_2O as the $Or_{26}Ab_{40}Q_{34}$ starting point, but in which $(Na_2O+K_2O)/Al_2O_3$ ranged up to 2.0. A similar constant-SiO_2, constant-Na_2O/K_2O series was mixed in which $(Na_2O+K_2O)/Al_2O_3$ ranged down to 0.67.

Because the evidence in rocks is not sufficient to conclude that $(Na_2O+K_2O)/Al_2O_3$ is the only composition variable affecting zircon solubility in felsic liquids, other major-element parameters were also investigated. In one case, a series of starting mixtures was made in which SiO_2 ranged from 68.0 to 78.5 wt.%, with

Table 1 (Continued)

	Series with variable Na/K											
	LN5		LN4		LN3		LN2		LN1		LN	
	mol%	wt.%	mol%	wt.%	mol%	wt.%	mol%	wt.%	mol%	wt.%	mol%	wt.%
SiO_2	84.12	78.63	84.12	78.47	84.13	78.34	84.13	78.20	84.13	78.04	84.13	77.90
Al_2O_3	6.62	10.50	6.62	10.48	6.62	10.46	6.62	10.44	6.62	10.42	6.62	10.40
Na_2O	5.38	5.19	4.99	4.80	4.63	4.45	4.28	4.10	3.88	3.71	3.52	3.36
K_2O	3.88	5.68	4.27	6.24	4.62	6.75	4.98	7.26	5.38	7.82	5.74	8.33
Alk/Al	1.40		1.40		1.40		1.40		1.40		1.40	
Na/K	1.39		1.17		1.00		0.86		0.72		0.61	

	Series with minor CaO and Fe_2O_3							
	PPK(g)		PK(g)		KPK(g)		K(g)	
	mol%	wt.%	mol%	wt.%	mol%	wt.%	mol%	wt.%
SiO_2	82.82	76.98	82.81	77.19	82.82	77.42	82.83	77.65
Al_2O_3	7.16	11.30	6.52	10.31	5.87	9.31	5.21	8.29
Fe_2O_3	0.40	1.00	0.40	1.00	0.40	1.00	0.40	1.00
CaO	1.15	1.00	1.15	1.00	1.15	1.00	1.14	1.00
Na_2O	5.25	5.03	5.65	5.43	6.06	5.84	6.45	6.24
K_2O	3.22	4.69	3.47	5.07	3.71	5.44	3.96	5.82
Alk/Al	1.18		1.40		1.66		2.00	
Na/K	1.63		1.63		1.63		1.63	

$(Na_2O+K_2O)/Al_2O_3$ constant at 1.18. An additional set of experiments incorporated variations in Na_2O/K_2O between 0.61 and 1.63, while SiO_2 and $(Na_2O+K_2O)/Al_2O_3$ were maintained at 84.1 mol% (~78 wt.%) and 1.40, respectively. In a final series of experiments aimed at more closely simulating natural granitic magmas, 1 wt.% each of CaO and Fe_2O_3 was introduced into starting materials of variable alkalinity, and the effects on zircon solubility were observed. The bulk compositions and relevant molar ratios for all experimental runs are summarized in Table 1.

Experimental and Analytical Techniques

Major oxide mixes of the starting materials were prepared from high-purity SiO_2 glass, reagent grade Al_2O_3, and pre-synthesized albite, leucite, sodium disilicate, or potassium disilicate (The identity of the alkali-bearing compounds in any given mix was determined by the desired ratio of alkalies/alumina). Mixes of these components were subjected to two cycles of grinding in an agate mortar (30 min) followed by heating at 1,300° C for 2 h. Only the highly peralkaline compositions melted completely at this temperature, but higher temperatures or longer heating times were not used because of the risk of alkali volatilization. For most experiments, zirconium was added to major oxide mixes as baddeleyite (ZrO_2) of 1–2 μm grain size, and a final 30-min mixing in agate was used to homogenize the powders. No subsequent high-temperature treatment was carried out because reaction of ZrO_2 and SiO_2 to form zircon in the starting materials was found to eliminate the possibility of attaining equilibrium in the actual experiments (Zircon is, in short, far less reactive in hydrous silicate melts than is ZrO_2; see following section of this paper). In the initial series of experiments, starting mixtures of each bulk composition were prepared with incremental amounts of added zirconium (usually 1,000, 2,000, 5,000, 10,000, and 20,000 ppm). As the systematic dependence of zircon solubility on melt composition became clearer, however, it was possible to estimate the level of Zr required to saturate the melt in zircon, and small incremental additions beginning at low levels were no longer necessary. For each experiment, 15 mg of starting material was sealed inside a gold capsule with 4 mg of distilled H_2O. The capsules were then inserted, in groups of 4–6, into conventional cold-seal pressure vessels and run for 6 to 30 days at 700°–800° C and 2.0 ± 0.1 kbar pressure. After quenching the pressure vessels in a stream of air, the charges were recovered and examined microscopically for presence or absence of zircon. [Confirmation of zircon identity by X-ray diffraction was possible when zircon abundance exceeded ~1%. Subordinate baddeleyite peaks were discernible in most X-ray patterns; because of the otherwise good evidence for equilibrium (see below), these peaks are attributed to isolated (and therefore inert) inclusions of ZrO_2 in zircon]. For a series of runs in which Zr was added in small increments to the same bulk composition, this simple microscopic inspection gave a good estimate of the Zr saturation level. Bulk Zr concentrations as low as 100 ppm produced occasional zircons in some runs; in such cases, the saturation level was considered simply to be <100 ppm. Most of the results reported in this paper are, however, for peralkaline compositions in which considerably higher Zr saturation levels exist. For these experiments, Zr concentrations in melts saturated with zircon were accurately determined by analysis of the quenched glasses with an electron microprobe.

The low-level microanalysis was greatly facilitated by the fact that any quenched glass containing a known amount of added, dissolved Zr (i.e., no zircon crystals present) could be used as a standard for determination of Zr concentrations in melts (glasses) saturated with zircon. A series of six such zircon-free glasses con-

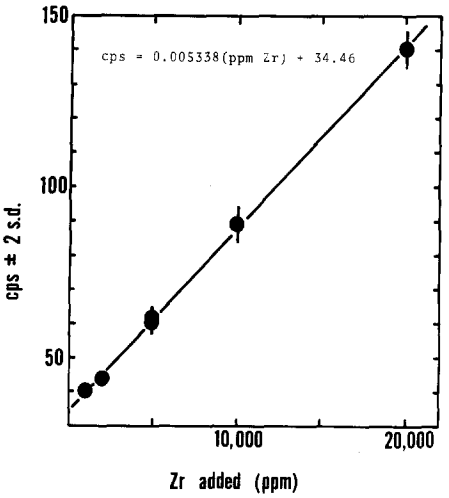

Fig. 1. Zirconium L_{α_1} X-ray intensity (*cps*) vs. amount of added Zr in six zircon-free glasses used as Zr standards (see Table 3 for identity of bulk compositions and Table 1 for oxide compositions). Error bars are ±2 standard deviations on 8 analysis spots

taining 1,000 to 20,000 ppm dissolved Zr was used to calibrate Zr L_{α_1} X-ray intensity vs. concentration as shown in Fig. 1, which serves to demonstrate both homogeneity of the glasses (see error bars) and probable accuracy of the weighed-in amounts of Zr[1]. The Zr L_{α_1} count rates shown in Fig. 1 were measured at 15 kV electron accelerating potential and 0.042 μA sample current, using a PET analyzing crystal. Relatively short count times (30 s) and a broad electron beam spot (~30 μm) were used in order to minimize damage to the surface of the water-bearing, alkali-rich glasses. The background count rate of 34±1 cps was confirmed both by counting on Zr-free glass at the peak position and by linear extrapolation of offset backgrounds on all standards and unknowns. For each unknown, Zr count rates were measured on 6–15 separate spots and the mean value was compared with the standard calibration (Fig. 1) to obtain a Zr concentration. Matrix corrections were found to be extremely small and were deemed unnecessary. X-ray counting data for all quenched glass unknowns are summarized in Table 2.

Table 2. X-Ray counting data

Zr in quenched glasses

Run no.	Bulk composition[a]	Mean cps	std dev (#pts)	Zr conc (ppm) ±2 SE
25	PK	119.06	2.7 (8)	15,849±355
30	PK	115.56	2.7 (8)	15,193±352
31	K	238.83	5.6 (8)	38,286±735
32	K	246.65	7.1 (8)	39,751±941
35	PK	115.94	2.8 (8)	15,264±372
44	PPK	68.59	1.8 (8)	6,394±241
44a	PPK	67.56	2.9 (8)	6,201±202
46	KPK	179.26	2.6 (8)	27,126±339
47	KPK	184.29	3.2 (8)	28,069±417
51	PPK	56.23	1.9 (8)	4,078±250
56	KPK	168.05	5.4 (8)	25,026±720
58	PPK	63.40	2.2 (8)	5,422±290
58a	PPK	64.00	4.3 (8)	5,533±278
59	PPK	50.36	1.5 (8)	2,979±195
60	PPK	34.21	1.8 (6)	–
45	KPK	142.71	1.2 (6)	19,675±165
57	KPK	173.82	4.1 (8)	25,261±436
61	K	250.55	7.4 (7)	39,041±933
62	KPK	197.11	10.2 (8)	29,445±1166
63	PK	124.19	8.0 (10)	16,347±712
64	PPK	81.57	9.6 (15)	8,694±490
72	LS	73.05	7.3 (12)	7,163±432
73	LS1	68.28	3.6 (10)	6,307±223
74	LS2	65.57	2.4 (10)	5,823±141
75	LS3	65.30	2.4 (10)	5,771±142
76	LS4	67.86	4.1 (10)	6,231±257
77	PPK(g)	54.48	2.3 (10)	3,829±112
78	PK(g)	105.94	4.6 (10)	13,070±370
79	KPK(g)	145.55	6.4 (10)	20,185±581
80	K(g)	199.22	5.9 (10)	29,823±629
81	LN	121.62	4.1 (9)	15,638±359
82	LN1	119.70	2.8 (8)	15,284±280
83	LN2	117.76	1.5 (8)	14,927±152
84	LN3	118.70	3.9 (8)	15,100±381
85	LN4	118.34	4.3 (9)	15,033±382
86	LN5	119.01	1.8 (8)	15,157±178

[a] See Table 1 for starting oxide compositions (not incl. ZrO_2) and Table 3 for run information

[b] Standardization shown in Fig. 1 applies to samples 25–60; two subsequent but nearly identical standardizations were used for remaining samples

Criteria for Equilibrium

Of major importance to any phase equilibrium study is a demonstration of equilibrium in at least some of the experiments performed. This is especially true of a system in which previous experimental results were viewed as suspicious even at the time they were presented (Dietrich, 1968). In the present study, an attempt was made to reverse some of the experiments by introducing small amounts of finely-ground natural zircon into some starting materials, with the hope that it would dissolve until the equilibrium amount of Zr in the melt was reached. In theory, this value should of course be the same as that obtained by crystallizing zircon from starting materials initially containing ZrO_2. Zircon was found, however, to be completely inert to solution in the melts for runs times as long as 4 weeks at 800° C[2], so an alternative demonstration of equilibrium was sought. One method was simply to compare the results of very long runs (30 days) with results of shorter runs made with the same starting materials. Such comparisons support the case for equilibrium, as there are no significant changes in apparent Zr saturation levels with time (Fig. 2a). Another argu-

[1] These glasses are available from the author in limited quantities for use as Zr standards

[2] This failure to dissolve zircon could explain the difficulties Dietrich (1968) had in obtaining equilibrium. His starting materials were gels, but these were pre-ignited several times at 550° C prior to loading the experimental capsules. Even very small amounts of zircon formed in these pre-ignitions would be difficult to dissolve in the experimental runs, especially at the 1 kbar water pressure used in that study

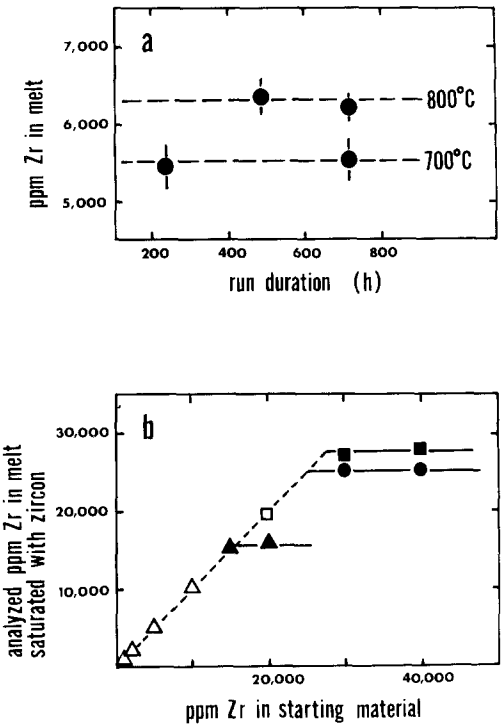

Fig. 2. a Analyzed ppm Zr in melts (glasses) saturated with zircon as a function of run duration. Run numbers 44 and 44a correspond to 800° points; 700° points represent runs 58 and 58a. Error bars are ±2 SE of the mean of 8 microprobe analysis spots. **b** Analyzed ppm Zr in glasses as a function of total Zr in the starting material. *Squares* and *circles* represent bulk composition KPK at 800° and 700° C, respectively; *triangles* represent composition PK at 800° C. *Solid symbols* indicate runs in which zircon was detected microscopically; *open symbols* designate charges lacking zircon

ment in favor of equilibrium is that the apparent Zr saturation level does not depend upon the amount of 'excess' zirconium added (Fig. 2b). If the quenched charges represent melts that have not reached equilibrium with contained zircon crystals, then it is difficult to envision why the level of dissolved zirconium in the melts should be independent of bulk zirconium concentration.

A final and perhaps most convincing attempt to demonstrate equilibrium was made by adding zirconium to the starting material as a compound other than ZrO_2. Metallic Zr (presumably highly reactive) was tried first, but was found to be impossible to crush and mix into the bulk oxide powder. The outcome was to use zirconium nitride [ZrN, synthesized by passing N_2 over hot (~1,300° C) zirconium powder] in combination with $AgNO_3$. These two compounds were mixed into starting materials in proportions appropriate for the following reaction to take place during melting:

$$3ZrN_{mix} + 2AgNO_{3\ mix} \rightarrow 3ZrO_{2\ melt,\ zircon} + 5/2N_{2\ gas} + 2Ag_{metal\ ppt}$$

Thus, in theory, the only chemical difference between these experimental charges and those in which Zr was added as ZrO_2 is nitrogen. This difference is considered to be of no consequence, and the ZrN-$AgNO_3$ experiments are thought to represent an alternate approach to zircon saturation, although obviously not a true reversal. Microscopic inspection of run products of charges initially containing ZrN and $AgNO_3$ revealed irregular silver metal blebs and zircon crystals much larger (up to 20 μm relative to 2–5 μm) and better-formed than those in the experiments initially containing ZrO_2. The difference in size and habit of the crystals suggests that the nucleation and growth mechanisms also are different: When Zr is added as ZrO_2, the baddeleyite grains act as nucleation sites for zircon, which grows by reaction of the baddeleyite with SiO_2 from the melt. In runs that initially contain Zr as ZrN, on the other hand, the smaller numbers of zircon nuclei (evidenced by fewer and larger crystals) probably indicate complete resorption of ZrN grains and subsequent homogeneous nucleation of zircon. In any case, the Zr contents of glasses surrounding the large zircons in the ZrN – $AgNO_3$ runs are similar to those in equivalent glasses containing zircons crystallized from ZrO_2 (Fig. 3). This agreement, in addition to the uniform distribution of Zr found in all the quenched glasses, is taken to mean that the experiments in general represent a close approach to equilibrium between zircon crystals and zirconium-bearing melts. Furthermore, the Zr concentrations in the melts are interpreted to be the levels at which zircon crystals would first appear in magmas undergoing gradual Zr enrichment from initially very low levels.

Results

Compositions in Which $(Na_2O+K_2O)/Al_2O_3 \leqq 1.0$

For all peraluminous bulk compositions, as well as the $Or_{26}Ab_{40}Q_{34}$ mixture, the level of zirconium required to saturate the melt in zircon is less than 100 ppm. This conclusion is reached because occasional zircons crystallize in charges containing 100 ppm total Zr and persist for run durations as long as 27 days (Table 3). (It should be noted that the peraluminous compositions, even at 800° C, contain minor amounts of corundum in addition to zircon, so the melts are not compositionally identical to the bulk starting materials. This fact does not invalidate the general conclusion that melts with excess alumina over alkalies can dissolve very little zirconium.) The observed low saturation level of Zr in $Or_{26}Ab_{40}Q_{34}$ is in agreement with Larsen's (1973) laser microprobe value of 57 ppm for $Or_{40}Ab_{15}Q_{45}$. In view of the minor effects of variations in SiO_2 and Na_2O/K_2O on Zr saturation levels (discussed below), this agreement would be predicted. In the present work, the inability to determine precise Zr concentrations in glasses containing less than ~500 ppm prompted more extensive experimentation with peralkaline compositions, in which zircon is far more soluble.

Compositions in Which $(Na_2O+K_2O)/Al_2O_3 > 1.0$

In Figs. 3–5, the zirconium concentrations in peralkaline melts saturated with zircon are plotted against the three primary composition parameters investi-

Table 3. Run data

$P_{H_2O} = 2$ kbar

Run no.	Bulk composition	ppm and form[a] of Zr in starting material	T° C	Run duration(h)	Phases in addition to vapor
1	P	1,000	680	144	gl+zc+occ qtz,flds
2	P	2,000	680	144	gl+zc+occ qtz,flds
3	P	5,000	680	144	gl+zc+occ qtz,flds
4	P	10,000	680	144	gl+zc+occ qtz,flds
5	P	20,000	680	144	gl+zc+occ qtz,flds
6	P	1,000	800	216	gl+zc
7	P	2,000	800	216	gl+zc
8	P	5,000	800	216	gl+zc
9	P	10,000	800	216	gl+zc[b]
10	P	20,000	800	216	gl+zc[b]
11	K	1,000	800	137	gl
12	K	2,000	800	137	gl
13	K	5,000	800	137	gl
14	K	10,000	800	137	gl
15	K	20,000	800	137	gl
16	K	1,000	700	142	gl
17	K	2,000	700	142	gl
18[s]	K	5,000	700	142	gl
19	K	10,000	700	142	gl
20[s]	K	20,000	700	142	gl
21[s]	PK	1,000	800	147	gl
22[s]	PK	2,000	800	147	gl
23[s]	PK	5,000	800	147	gl
24[s]	PK	10,000	800	147	gl
25	PK	20,000	800	147	gl+zc
26	PK	1,000	700	288	gl
27	PK	2,000	700	288	gl
28	PK	5,000	700	288	gl
29	PK	10,000	700	288	gl
30	PK	20,000	700	288	gl+zc
31	K	50,000	700	288	gl+zc
32	K	50,000	800	163	gl+zc[b]
33	P	200	800	163	gl+occ zc
34	P	500	800	163	gl+occ zc
35	PK	15,000	800	163	gl+occ zc
36	M	500	800	284	gl+cor+zc
37	M	1,000	800	284	gl+cor+zc
38	M	2,000	800	284	gl+cor+zc
39	M	5,000	800	284	gl+cor+zc[b]
40	P	1,000	800	487	gl+zc
41	P	10,000	800	487	gl+zc
42	P	20,000	800	487	gl+zc[b]
43	PPK	5,000	800	487	gl
44	PPK	10,000	800	487	gl+zc
44a	PPK	10,000	800	719	gl+zc
45	KPK	20,000	800	382	gl
46	KPK	30,000	800	382	gl+zc
47	KPK	40,000	800	382	gl+zc
48	PM	200	800	382	gl+occ cor,zc
49	PM	500	800	382	gl+zc+occ cor
50	PPK	5,000 as zircon	800	648	gl+zc
51	PPK	8,000(3,000 as zircon)	800	648	gl+zc
52	P	100	800	648	gl+occ zc
53	P	200	800	648	gl+occ zc
54	P	20,000	800	648	gl+zc[b]
55	PM	100	800	648	gl+occ zc,cor

Table 3 (continued)

Run no.	Bulk composition	ppm and form[a] of Zr in starting material	$T°$ C	Run duration (h)	Phases in addition to vapor
56	KPK	30,000	700	238	gl+zc
57	KPK	40,000	700	238	gl+zc
58	PPK	10,000	700	238	gl+zc
58a	PPK	10,000	700	719	gl+zc
59	PPK	8,000(3,000 as zircon)	700	238	gl+zc
60	PPK	5,000 as zircon	700	238	gl+zc
61	K	50,000 as ZrN	700	264	gl+zc
62	KPK	40,000 as ZrN	700	264	gl+zc
63	PK	20,000 as ZrN	700	264	gl+zc
64	PPK	20,000 as ZrN	700	264	gl+zc
65	P	100 as ZrN	700	264	gl+occ zc
66	P	20,000 as ZrN	700	264	gl+zc
67	LS	20,000	700	239	gl+zc+flds
68	LS1	20,000	700	239	gl+zc+flds
69	LS2	20,000	700	239	gl+zc+flds
70	LS3	20,000	700	239	gl+zc+occ flds
71	LS4	20,000	700	239	gl+zc+occ flds
72	LS	20,000	800	168	gl+zc
73	LS1	20,000	800	168	gl+zc
74	LS2	20,000	800	168	gl+zc
75	LS3	20,000	800	168	gl+zc
76	LS4	20,000	800	168	gl+zc
77	PPK(g)	10,000	700	188	gl+zc+occ flds
78	PK(g)	30,000	700	188	gl+zc+occ flds
79	KPK(g)	40,000	700	188	gl+zc+occ flds
80	K(g)	50,000	700	188	gl+zc+occ flds
81	LN	25,000	750	190	gl+zc
82	LN1	25,000	750	190	gl+zc
83	LN2	25,000	750	190	gl+zc
84	LN3	25,000	750	190	gl+zc
85	LN4	25,000	750	190	gl+zc
86	LN5	25,000	750	190	gl+zc

Abbreviations: gl: glass; *zc*: zircon; *qtz*: quartz; *flds*: feldspar; *cor*: corundum; *occ*: occasional

s: Used as a standard in microprobe analysis (see text)

[a] ZrO_2 unless otherwise specified

[b] Zircon identified by XRD; subordinate peaks of unreacted(?) baddeleyite also observed in some cases

gated, namely molar $(Na_2O+K_2O)/Al_2O_3$ (Fig. 3), SiO_2 concentration (Fig. 4), and Na_2O/K_2O (Fig. 5). Before discussing these figures in detail, it is important to note that temperature has little or no effect on zircon solubility. This is clear in Fig. 3, which shows near coincidence of data points representing experiments at 700° and 800° C. For runs initially containing Zr as ZrO_2, slightly higher Zr saturation levels are apparent in the 800° runs relative to those at 700°. However, the significance of this difference is questionable because the results of experiments at 700° on starting materials containing ZrN are nearly identical with those for the 'ZrO_2' experiments at 800°. In any case, the effect of temperature is small, and is disregarded in remaining sections of this paper.

Variations in $(Na_2O+K_2O)/Al_2O_3$. A pronounced dependence of zircon solubility in felsic liquids upon the molar ratio $(Na_2O+K_2O)/Al_2O_3$ is revealed in Fig. 3, in which all plotted points represent liquids of the same molar SiO_2 concentration (84.1%, neglecting SiO_2 consumed by growth of zircons) and Na_2O/K_2O value (1.63). The change in $(Na_2O+K_2O)/Al_2O_3$ of the liquids from 1.0 to 2.0 is accompanied by a $\sim$500-fold increase ($<$100 ppm to almost 4 wt.%) in Zr content of melts coexisting with zircon. This increase appears to be linear, so the lines shown for each series of runs are linear least-squares fits to the data, constrained to pass through 100 ppm Zr at $(Na_2O+K_2O)/Al_2O_3=1.0$. Most data points fall on or close to the least-squares

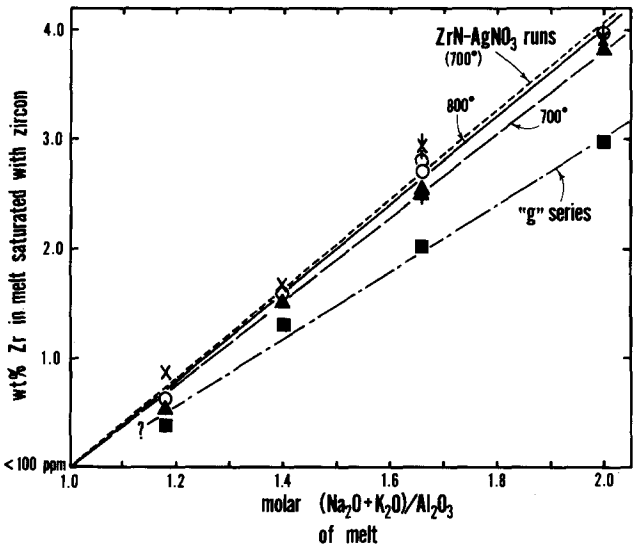

Fig. 3. Weight per cent dissolved Zr in melts saturated with zircon vs. molar $(Na_2O+K_2O)/Al_2O_3$ of the melts. *Circles* and *triangles* represent runs at 800° and 700° C, respectively, in which Zr was added initially as ZrO_2. X show values for 700° C runs in which Zr was introduced as ZrN. *Squares* are results of experiments on bulk compositions containing 1 wt.% each of CaO and Fe_2O_3 (*"g" – series*). *Lines* are least squares fits; error bars are ±2 standard errors of the mean microprobe analysis value. See text for further explanation

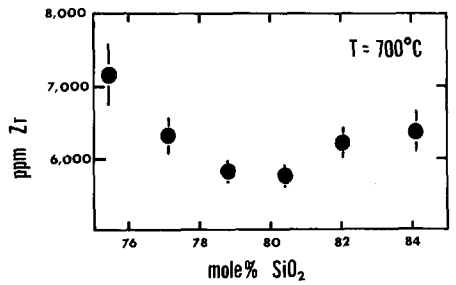

Fig. 4. Dissolved Zr (ppm) in melts saturated with zircon as a function of molar SiO_2 concentration in the melts. Molar $(Na_2O+K_2O)/Al_2O_3$ of the melts is the same (i.e., 1.18) for all runs represented. Error bars are ±2 standard errors

lines, although at $(Na_2O+K_2O)/Al_2O_3=1.18$ they appear to be systematically low for starting materials containing ZrO_2, and high for the run initially doped with ZrN. The mean value for runs using the two starting compounds is, however, well represented by the linear fit, so this is assumed to be the true equilibrium value (~7,250 ppm).

Variations in SiO_2 Concentration. In Fig. 4 are shown the results of a series of experiments in which both $(Na_2O+K_2O)/Al_2O_3$ and Na_2O/K_2O of the melts were held constant at 1.18 and 1.63, respectively, but in which the SiO_2 concentration was varied from 75.5

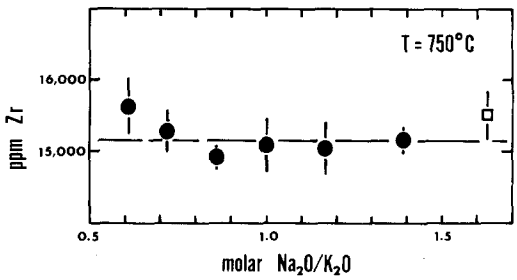

Fig. 5. Dissolved Zr (ppm) in melts saturated with zircon as a function of Na_2O/K_2O of the melts. Molar $(Na_2O+K_2O)/Al_2O_3$ of the melts is 1.40 in all runs; SiO_2 concentration is also constant at 84.1 mol%. Error bars are ±2 SE

to 84.1 mol% (68.0–78.6 wt.%). The range of observed Zr concentrations in six melts coexisting with zircon is 5,800 to 7,200 ppm, with no apparent systematic dependence upon melt SiO_2 content (the plot has a minimum at about 80 mole% SiO_2).

Compared with the changes induced by variations in $(Na_2O+K_2O)/Al_2O_3$, the influence of SiO_2 concentration on zircon saturation is extremely small, and may in fact be non-existent over the range in SiO_2 level investigated. When the error bars in Fig. 4 are taken into consideration along with the difference in apparent saturation levels obtained by adding Zr as ZrO_2 and ZrN (Fig. 3), the 1,400 ppm range of Zr concentration values shown in Fig. 4 seems small indeed, and perhaps insignificant for the particular peralkaline series studied. The question must remain open as to whether SiO_2 concentration is important to zircon solubility in subaluminous and peraluminous liquids, but for peralkaline compositions it is clearly a secondary influence at most[3]. Moreover, because SiO_2 cannot be varied independently of the concentrations of the other three components (Na_2O, K_2O, and Al_2O_3), it can be concluded that changes in the absolute amounts of alkalies or alumina do not significantly affect the level of dissolved ZrO_2 required to saturate a melt in zircon.

Variations in Na_2O/K_2O. The effect on zircon solubility of large variations in Na_2O/K_2O(0.61–1.63) is shown in Fig. 5 for a series of seven melts with constant $(Na_2O+K_2O)/Al_2O_3$ (i.e., 1.40) and constant molar amounts of SiO_2 (84.1%) and Al_2O_3 (6.62%). As in the case of the variable – SiO_2 runs, this series shows a small range in Zr saturation level (1.49–1.56 wt.%), indicating little or no influence of Na_2O/K_2O. The error bars shown are ±2 SE of the mean; the use of ±3 SE would allow a horizontal

[3] This knowledge should dismiss any speculations regarding the effects of small changes in SiO_2 concentration of the melts due to crystallization of zircon from them

line at 1.52 wt.% Zr to pass through all of the error bars.

The Effect of Minor Amounts of CaO and Fe_2O_3. Included in Fig. 3 are data points (squares) for runs whose bulk compositions are similar to the others represented in the figure except that 1 wt.% each of CaO and Fe_2O_3 was added to the starting materials. A linear least-squares fit through four points is shown, with the realization that there is relatively little justification for such a fit. As discussed later in this paper, the trend of these data points, unlike those of the other series represented, is not necessarily constrained to pass through ~100 ppm Zr at $(Na_2O+K_2O)/Al_2O_3=1.0$. For the moment, it is sufficient to note a shift from the Ca-, Fe-free trends corresponding to a ~25% reduction in Zr saturation level for any given value of $(Na_2O+K_2O)/Al_2O_3$. The saturation level is still strongly dependent upon $(Na_2O+K_2O)/Al_2O_3$, attaining a value of 3 wt.% Zr at $(Na_2O+K_2O)/Al_2O_3=2.0$.

Geochemical Applications

From the experimental results reported above emerges a relatively simple picture of the petrologic/geochemical conditions appropriate for zircon crystallization from felsic magmas. Only two variables are of major importance in determining whether a magma is saturated in zircon: these are (1) the amount of Zr present in the system, and (2) the $(Na_2O+K_2O)/Al_2O_3$ ratio of the liquid. A surprisingly small, and probably negligible, influence can be expected from variables such as temperature, SiO_2 content, and Na_2O/K_2O of the magma over the ranges of these parameters observed in natural felsic systems. The fact that the experimental charges were all water-saturated, whereas felsic magmas may not be, is not, for reasons discussed in the last section of this paper, regarded as a serious limitation.

Zircon Crystallization in Subaluminous and Metaluminous Magmas

Because of the extremely low solubility of zircon in non-peralkaline melts, it seems likely that zircon is a liquidus phase in most felsic magmas lacking normative alkali silicate and acmite [the range of Zr concentrations in granitic rocks is 50–700 ppm (Chao and Fleischer, 1960), with an average value of 170 ppm (Turekian and Wedepohl, 1961)]. Zirconium concentrations greater than 100 ppm in felsic, non-peralkaline rocks almost certainly do not represent Zr abundances in *liquids*, but some composite value of melt + zircon crystals. The extent of actual removal of zircon from a given felsic magma will in most cases be difficult or impossible to estimate. It can, however, be presumed to be large in the case of granitic magmas that are demonstrably produced by fractional crystallization of mafic precursors, and yet contain little zirconium. This is true because Zr shows generally incompatible behavior toward principal magmatic minerals, and extensive crystal fractionation would lead to its enrichment in derivative liquids unless zircon were removed at some stage.

Residual Zircon in Crustal Fusion Episodes

The low measured zircon solubility in melts that are not peralkaline brings up the interesting likelihood that this minor mineral is a residual phase in regions of the Earth's crust that have undergone partial melting. This possibility was considered briefly by Buma et al. (1971), who pointed out the implications of residual zircon to bulk rock/melt partition coefficients for elements such as the REE and Ta. These authors, however, lacked the necessary data for detailed calculations of the effect of residual zircon. For the present purposes, it is instructive to consider quantitatively the behaviour of REE in a hypothetical partial melting situation in which zircon is not consumed. A source rock of granitic mineralogy is assumed ($^1/_3$ quartz, $^1/_3$ sodic plagioclase, $^1/_3$ K-spar), and is assigned the following initial trace element characteristics: 300 ppm Zr; 200, 40, and 20 times chondrite values for Ce, Gd, and Lu, respectively[4] (Because measured partition coefficients are available for Ce, this element, rather than La, was used as a representative light REE). The problem is reduced to its simplest terms by the following assumptions: (1) any subordinate ferromagnesian minerals present to not contain significant proportions of the total REE in the system; (2) the feldspars, quartz, and ferromagnesian minerals do not contain significant amounts of Zr; (3) except for zircon, the minerals melt in equal proportions; and (4) an equilibrium distribution of REE between melt and residual rock is attained in all cases. Solid/liquid partition coefficients (and solid/solid values calculated from them) were obtained from the literature (see Table 4). Because of the uncertainties in selection of partition coefficients for Eu, no attempt was made to model the behavior of this element;

[4] These REE abundances closely resemble those in high-grade South African felsic gneisses studied by McCarthy and Kable (1978), and are qualitatively similar to Australian post-Archean sediments and the North American shale composite (Nance and Taylor, 1976)

Table 4. Crystal/liquid partition coefficients

	Ce	Gd	Lu
Quartz	0	0	0
K-feldspar[a]	0.04	0.01	0.01
Plagioclase[a,b]	0.12	0.08	0.04
Zircon[c]	1	10	400

[a] Schnetzler and Philpotts (1970)
[b] Nagasawa and Schnetzler (1971)
[c] Nagasawa (1970)

rather, the REE were treated as a coherent group exhibiting smoothly changing partition coefficients from Ce to Lu.

In Figs. 6 and 7a, the initial distribution of REE in minerals of the source rock is shown. Of particular interest is the fact that, even in a rock containing only 300 ppm Zr (0.06 wt.% zircon), a large proportion of the heavy REE is located in zircon (e.g., ~93% of total Lu). Figure 7b illustrates the case of 10% equilibrium melting when the melt is saturated in zircon at the realistic value of 60 ppm dissolved Zr[5]. Here the melt shows an average ~tenfold enrichment in REE relative to the initial source rock. Due to their retention by zircon in the residue, the heavy REE exhibit slightly less enrichment in the melt than do the light REE. This fractionation is more obvious in the REE pattern of the residue itself, which drops significantly below the curve for the initial source except at the heavy end. If equilibrium melting progresses to 40% (Fig. 7c), the residue curve develops a pronounced 'sag' in the middle due to loss of the intermediate and light REE to the melt; the Lu value, however, remains nearly fixed just above 10 times chondrites.

The figures discussed above (7b and c) clearly illustrate the effect of residual zircon on REE distributions during crustal melting episodes. The most obvious consequence is heavy REE enrichment in the unmelted residue, manifested as a U- or V-shaped REE pattern. This pattern contrasts with the heavy REE-depleted pattern inherited by a residue without zircon (Fig. 7d). Because of the specific assumptions made in producing Fig. 7, it is not expected that any given natural example of partial melting in the crust will result in curves identical to those shown. The initial source-rock mineralogy and REE characteristics, as well as the extent of REE equilibration between melt and residual crystals, will influence the nature of the curves. If the source rock were extremely enriched in light relative to heavy REE, for example,

[5] Peralkaline liquids would not be expected in partial fusion of feldspar + qtz ± mica assemblages

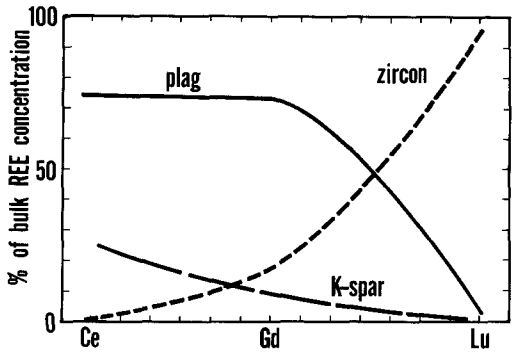

Fig. 6. Plot showing % of bulk REE concentration in each mineral of the model source rock used to produce Fig. 7. See text

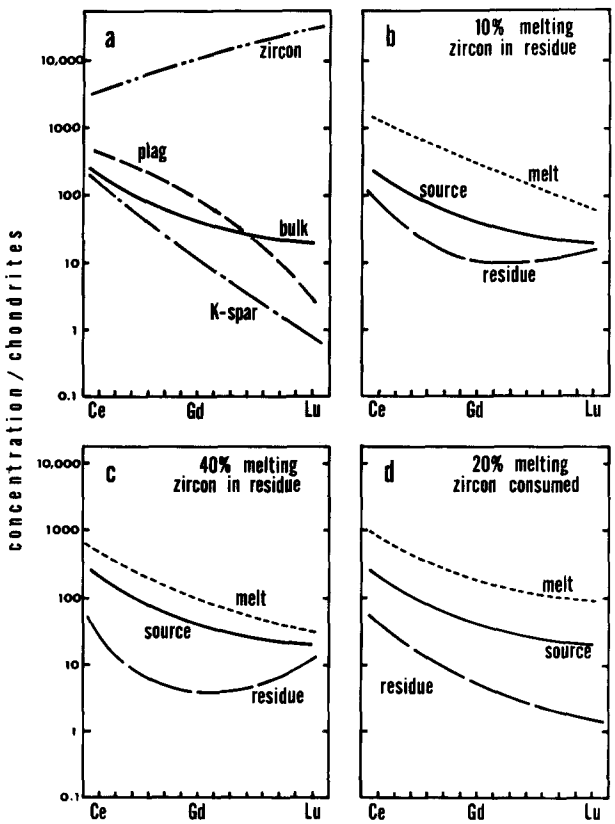

Fig. 7. **a** Distribution of REE in the minerals of a source rock consisting of $^1/_3$ quartz, $^1/_3$ K-feldspar, $^1/_3$ sodic plagioclase, and 0.06 wt.% zircon (300 ppm Zr). Bulk rock distribution curve is shown for reference. See Table 4 for solid/liquid partition coefficients from which the solid/solid values were calculated. See text for further explanation. **b–d** Distribution of REE in melt and residue produced by equilibrium melting of the source rock whose initial REE characteristics are shown in Figs. 6 and 7a. In **b** and **c** the melt is assumed to be saturated in zircon at 60 ppm dissolved Zr; under these circumstances, the zircon abundances in the residues are 0.066 and 0.092 wt.% for **b** and **c**, respectively. In **d**, zircon is considered to be consumed by 20% equilibrium melting, resulting in an unrealistically high value of 1,500 ppm dissolved Zr in the melt. See text for further discussion and assumptions regarding all models

the pattern of the residue would assume a 'backwards J' shape as melting progressed, rather than the U shape shown in Fig. 7c. Any evaluation of the possibility of melting in the presence of zircon should include measurements of Zr concentration in the alleged melts. According to the experimental data, crustal rocks containing >60 ppm Zr, regardless of the extent to which they are melted, can only yield melts that are saturated in zircon. As melting progresses in a region containing >60 ppm Zr (initially as zircon), the total abundance of zircon in the system decreases, the proportion of zircon in the residue increases, and the concentration of Zr in the liquid is buffered at a constant, low value (i.e., ~60 ppm). Such a value should be observed in magmatic rocks whose origins involve partial fusion in the crust. The natural case, of course, will seldom be as simple as that just described. A likely complicating factor is actual entrainment of zircon crystals by a migrating melt fraction, a process that may in fact be widespread in situations where the degreee of melting is high.

Peralkalinity and Zircon Crystallization

As noted in the introduction, there is ample evidence in rocks that peralkaline liquids retain large concentrations of Zr in solution. Nicholls and Carmichael (1969) present the most convincing evidence in this regard: These authors determined that the ~1,800 ppm of Zr contained in certain pantellerites is uniformly distributed in the glassy matrix. [In contrast, Carmichael and McDonald (1961) noted occasional zircon crystals in metaluminous obsidians containing as little as 200–300 ppm total Zr.] There is, in short, a long-recognized positive correlation between acid rock alkalinity and Zr concentration that is not attributable to zircon abundance. The present experimental results not only confirm the apparent relationship between zircon solubility and magma alkalinity, but also make possible the ensuing quantitative treatment of zirconium/zircon behavior in alkaline magmas.

Peralkaline acid magmas, as represented by comendites and pantellerites and their intrusive equivalents, are generally held to be derivatives of trachytic liquids (Carmichael and MacKenzie, 1963; Siedner, 1965). The specific mechanism that relates a liquid exhibiting a molar excess of alkalies over alumina to a precursor that has no such excess is fractional crystallization of a calcium-bearing alkali felspar (Carmichael and MacKenzie, 1963). This mechanism, termed the 'plagioclase effect' by Bowen (1945) in reference to potassium-free systems, can be simply understood as the failure of pure alkali feldspar to

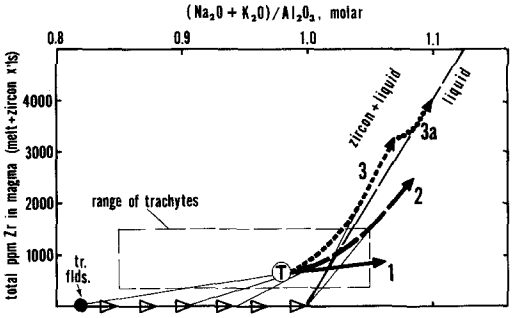

Fig. 8. Diagram ilustrating possible paths for the evolution of trachytic magma (T) in terms of Zr abundance and $(Na_2O+K_2O)/Al_2O_3$ that can result from fractional crystallization of feldspar. See text for explanation

precipitate from a melt that contains calcium. In Fig. 8, some models of the evolution of peralkaline magmas with respect to zircon saturation are put forth. All of these models assume a parental trachytic magma ('T' in Fig. 8) that precipitates an alkali felspar initially containing 10 wt.% An component [~2 wt.% CaO; $(Na_2O+K_2O)/Al_2O_3=0.82$]. This particular feldspar was chosen from the data summarized by Tuttle and Bowen (1958, p. 132) as a composition typical of the high-calcium alkali feldspar phenocrysts found in trachytes. The position of the trachytic magma itself in Fig. 8 is arbitrary but realistic, and in any case not critical to the arguments. The large rectangular box surrounding point T on the diagram represents the range of Zr concentrations and $(Na_2O+K_2O)/Al_2O_3$ values for all oceanic-island trachyte analyses listed in Carmicheal et al. (1974). The experimental data require that the trachyte at T, which contains ~600 ppm Zr, be saturated in zircon. Path 1 in Fig. 8 shows the change in Zr content and $(Na_2O+K_2O)/Al_2O_3$ for magmas produced by up to 35% removal from the trachyte of a feldspar of constant high CaO (2 wt.%). [Note that the plotted Zr values in Fig. 8 are total ppm in the magma. Clearly, where zircon is stable, this is a composite value of Zr in zircons plus that dissolved in the melt. The particular paths discussed here (except for 3a) show the effects of feldspar fractionation only, and do not consider the possible gravitational removal of zircon from those magmas in which it is stable]. After 20% feldspar crystallization, the magma has become sufficiently peralkaline that zircon becomes unstable (i.e., the zircon saturation curve is crossed). Path 2 shows a more realistic situation in which the felspar adjusts to lower-CaO compositions as CaO is removed from the melt. In this case, derivative magmas follow an upward-curving trajectory until the feldspar reaches an essentially Ca-free composition, at which time the path becomes

nearly straight and away from a feldspar of $(Na_2O+K_2O)/Al_2O_3=1.0$ (the path is not exactly linear because the abscissas are ratios). The important point concerning paths 1 and 2 is that, once zircon becomes unstable due to the increase in peralkalinity, the melt can *never* regain zircon saturation by continued feldspar crystallization. Thus, Zr enrichment in the melt to very high values is possible. Re-crossing the zircon saturation line can only be achieved by precipitation of, for example, an alkali-rich pyroxene or amphibole.

The remaining possible type of path in Fig. 8 is represented by curve 3. In this case, the interval over which Ca-rich feldspar precipitates is small enough that derivative magmas do not reach sufficient alkalinity to dissolve zircons present in the original trachyte. These magmas are destined to remain saturated in zircon. Continued (pure alkali) feldspar removal will produce magmas of progressively higher peralkalinity, but the path will remain in the zircon + liquid field. This long-term saturation in zircon brings up the possibility of complete gravitational removal of zircons from the system, a case that is represented by path 3a.

The magma evolution curves discussed in reference to Fig. 8 are selected special cases that *could* apply to real magmatic situations. The evolution of magmas may of course be subject to other variables not considered in drawing the simple curves. In view of the measured effect of minor amounts of Ca and Fe upon zircon solubility, for example, the slope of the saturation line itself is somewhat in question. Fractional crystallization of zircon, not taken into account in curves 1–3, could substantially alter the magma evolution paths. Even the position of the parental magma (T) is, as previously noted, arbitrary. For the present purposes, all of these potential modifying factors are considered to be unimportant, not because they are inoperative or unknown, but because they cannot change the conclusions regarding the *types* of magma evolution paths that are possible.

Concluding Remarks: Evidence for Zirconium Complexing in Magmas

One remaining task that falls within the scope of this paper is to explain the marked dependence of the zircon saturation level in felsic melts upon $(Na_2O+K_2O)/Al_2O_3$. The fact that zircon solubility is extremely low in melts that do not have an excess of alkalies over alumina is an obvious clue to an explanation. In Fig. 9, the cation % of Zr in melts saturated with zircon is plotted against the molar

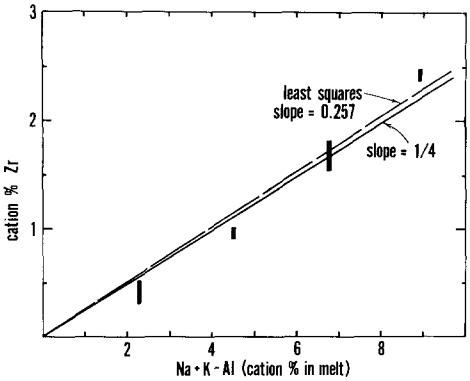

Fig. 9. Cation % Zr in peralkaline melts coexisting with zircon plotted against the abundance of alkalies not associated with Al^{3+} in the melt. The data do not define a straight line, but do fall close to the indicated line of *slope* $=1/4$. *Dashed line* is a least squares fit to the data, constrained to pass through the origin. See text

excess of alkalies over aluminum (i.e., Na + K-Al) in the melts. The total range of measured Zr saturation values for each melt composition is shown (These include 700° and 800° runs and 'reversed' experiments, but not those runs in which Ca and Fe were added). The near coincidence of the trend with a line of slope $=1/4$ suggests that there is indeed a simple relationship between the amount of dissolvable ZrO_2 and the abundance of alkalies over alumina: for every two moles of 'excess' M_2O in the melt, one mole of ZrO_2 will dissolve, This is interpreted to mean that molecules or complexes exist in the melt in which $M_2O/ZrO_2=2$. Because there are no known discrete alkali zirconate ions (Cotton and Wilkinson, 1972), it is reasonable to conclude that the species are alkali zircono-silicates, possibly of $M_4Zr(SiO_4)_2$ stoichiometry. The exact nature of the zircono-silicate complexes cannot be determined, but because zircon solubility does not depend upon Na/K, it seems clear that the existence of the complexes is insensitive to this ratio. Apparently, however, the complexes cannot incorporate alkalies that are associated with aluminum in feldspar-like molecules.

Because of the somewhat decreased solubility of zircon that is observed in melts containing minor amounts of Ca and Fe (Fig. 3), it is concluded that one or both of these elements interferes with the alkali-zirconium complexing that occurs in the simple 4-component melts. This possibility could be further investigated by separate systematic additions of Ca and Fe, accompanied by measurement of ferric iron content of the run products. The outcome of such a study would probably be that zircon solubility is linearly related to $Na+K-Al-Fe^{3+}$, at least

for Ca-free compositions[6]; in other words, alkali complexing with Al *and* with Fe^{3+} takes place in preference to alkali-zirconosilicate complexing. Only the alkalies 'left over' after 1:1 combination with Al and Fe^{3+} would be free to form zirconosilicate units. [For this reason, the trend of Fe-bearing compositions in Fig. 3 would not be expected to pass through ~60 ppm Zr at $(Na_2O+K_2O)/Al_2O_3=1.0$]. The intent of introducing Ca and Fe into some of the present experiments was simply to establish that felsic magmas, which contain minor amounts of these elements, show zircon saturation levels that are qualitatively similar to those observed in the simple $Na_2O - K_2O - Al_2O_3 - SiO_2 - H_2O$ system.

A final point regarding the applicability of the experimental data to magmas is that, whatever the exact role of K_2O and Na_2O in stabilizing Zr^{4+} in the melt, it cannot be filled by H_2O. The parameter that controls zircon solubility is clearly not $(Na_2O+K_2O+H_2O)/Al_2O_3$. Water-saturated compositions lacking an abundance of alkalies over alumina can dissolve < 100 ppm Zr – it does not seem likely that the saturation level could be much lower in water-undersaturated melts. Furthermore, water does not seem to be critical to the high solubility of zircon in peralkaline liquids: As previously noted, Nicholls and Carmichael (1969) measured high concentrations of Zr in pantellerite glasses, which are at least water-undersaturated, if not altogether dry (Carmichael and MacKenzie, 1963). For these reasons, it is believed that the experimental data presented in this paper can be applied with confidence to rocks.

Acknowledgments. This paper benefited from the constructive preliminary reviews of C. Capobianco, F. Frey, C. Langmuir, and M. Loiselle. The research was supported in part by the Department of Geology, Rensselaer Polytechnic Institute and in part by the Earth Sciences Section, National Science Foundation, NSF Grant EAR-7812980.

References

Bowden, P.: Zirconium in Younger Granites of Northern Nigeria. Geochim. Cosmochim. Acta **30**, 985–993 (1966)

Bowen, N.L.: Phase equilibria bearing on the origin and differentiation of alkaline rocks. Am. J. Sci. **243A**, Daly vol., 75–89 (1945)

Buma, G., Frey, F.A., Wones, D.R.: New England granites: Trace element evidence regarding their origin and differentiation. Contrib. Mineral. Petrol. **31**, 300–320 (1971)

Carmichael, I.S.E., McDonald, A.: The geochemistry of some natural acid glasses from the North Atlantic tertiary volcanic province. Geochim. Cosmichim. Acta **25**, 189–222 (1961)

Carmichael, I.S.E., MacKenzie, W.S.: Feldspar-liquid equilibria in pantellerites: An experimental study. Am. J. Sci. **261**, 382–396 (1963)

Carmichael, I.S.E., Turner, F.J., Verhoogen, J.: Igneous petrology. New York: McGraw-Hill Book Company 1974

Chao, E.C.T., Fleischer, M.: Abundance of zirconium in igneous rocks. Rept. 21st Intern. Geol. Congr. Norden, Part 1. pp. 106–131 (1960)

Cotton, F.A., Wilkinson, G.: Advanced inorganic chemistry. New York: John Wiley Interscience 1972

Dietrich, R.V.: Behavior of zirconium in certain artificial magmas under diverse P-T conditions. Lithos **1**, 20–29 (1968)

Goldschmidt, V.M.: Geochemistry. Oxford: Clarendon Press 1954

Larsen, L.: Measurement of solubility of zircon ($ZrSiO_4$) in synthetic granitic melts. Eos. **54**, 479 (1973)

McCarthy, T.S., Kable, E.J.D.: On the behavior of rare-earth elements during partial melting of granitic rock. Chem. Geol. **22**, 21–29 (1978)

Nagasawa, H.: Rare earth concentrations in zircons and apatites and their host dacites and granites. Earth Planet. Sci. Lett. **9**, 359–364 (1970)

Nagasawa, H., Schnetzler, C.C.: Partitioning of rare earth, alkali and alkaline earth elements between phenocrysts and acidic igneous magma. Geochim. Cosmochim. Acta **35**, 953–968 (1971)

Nance, W.B., Taylor, S.R.: Rare earth element patterns and crustal evolution – I. Australian post-Archean sedimentary rocks. Geochim. Cosmochim. Acta **40**, 1539–1552 (1976)

Nicholls, J., Carmichael, I.S.E.: Peralkaline acid liquids: A petrological study. Contrib. Mineral. Petrol. **20**, 268–294 (1969)

Nockolds, S.R., Allen, R.: The geochemistry of some igneous rock series. Geochim. Cosmochim. Acta **4**, 105–142 (1953)

Poldervaart, A.: Zircon in rocks. 2. Igneous rocks. Am. J. Sci. **254**, 521–554 (1956)

Schnetzler, C.C., Philpotts, J.A.: Partition coefficients of rare earth elements between igneous matrix material and rockforming mineral phenocrysts – II. Geochim. Cosmochim. Acta **34**, 331–340 (1970)

Siedner, G.: Geochemical features of a strongly fractionated alkali igneous suite. Geochim. Cosmochim. Acta **29**, 113–137 (1965)

Turekian, K.K., Wedepohl, K.H.: Distribution of the elements in some major units of the Earth's crust. Geol. Soc. Am. Bull. **72**, 175–192 (1961)

Tuttle, O.F., Bowen, N.L.: Origin of granite in light of experimental studies in the system $NaAlSi_3O_8 - KAlSi_3O_8$-SiO_2. Geol. Soc. Am. Mem. **74**, 153pp. (1958)

Wager, L.R., Mitchell, R.L.: The distribution of trace elements during strong fractionation of basic magmas: a further study of the Skaergaard intrusion. Geochim. Cosmochim. Acta **1**, 129–209 (1951)

[6] If Fig. 3 is re-plotted with Al_2O_3 concentration replaced by the sum $Al_2O_3+Fe_2O_3$ (assuming any added iron to be entirely ferric), the compositions containing Ca and Fe are still slightly displaced from the trend of Ca-, Fe-free experiments. It seems likely, therefore, that Ca has some influence on zircon solubility

Received May 29, 1979; Accepted in revised form July 24, 1979